Health, 2025, 17(2), 98-110
https://www.scirp.org/journal/health
ISSN Online: 1949-5005
ISSN Print: 1949-4998

An Antimicrobial and Antioxidant Hydrogel Dressing for Wound Repair

Xiaochun Liu[1,2], Hui Zhang[2,3*], Dawei Sun[2], Lei Xu[2]

[1]The Second School of Clinical Medicine, Southern Medical University, Guangzhou, China
[2]Department of Orthopedics, Guangdong Second Provincial General Hospital, Guangzhou, China
[3]Department of Orthopedics, Southern Medical University, Guangzhou, China
Email: 254819792@qq.com, *17732503722@163.com

How to cite this paper: Liu, X.C., Zhang, H., Sun, D.W. and Xu, L. (2025) An Antimicrobial and Antioxidant Hydrogel Dressing for Wound Repair. *Health*, **17**, 98-110.
https://doi.org/10.4236/health.2025.172007

Received: December 26, 2024
Accepted: February 9, 2025
Published: February 12, 2025

Abstract

The management of chronic wounds remains a substantial challenge for healthcare providers. Inadequate wound care can result in serious complications, including infection, which may ultimately lead to amputation or even death. While traditional excipients exhibit some efficacy in promoting wound healing, they are not sufficiently effective in preventing wound infections. As an antimicrobial metal, copper has a long history in the antimicrobial field, and at the same time, wound auxiliaries with copper ions have also been used in the treatment of chronic wounds. To address the limitations of conventional wound dressings, including insufficient antimicrobial properties and limited capacity to promote wound healing, this study introduces a highly adhesive hydrogel with superior mechanical stability for non-invasive wound treatment. The hydrogel was composed of carboxymethyl chitosan, tannic acid and copper ions. The tannic acid solution was subjected to dropwise addition of $CuCl_2$ solution to produce precipitation, and tannic acid/copper ions (TA/Cu^{2+}) composite nanoparticles were prepared. Through topological adhesion, the CMCS with pH sensitivity has the ability to establish adhesive connections with a wide range of materials. The benefits of $CMCS/TA/Cu^{2+}$ hydrogel, as a kind of wound closure and repair material, include efficient wound closure, and resistance against bacterial invasion while maintaining cleanliness. Additionally, it exhibits excellent tensile and mechanical stability that can facilitate effective closure and repair in dynamic areas like joint wounds. This promising hydrogel adhesive has demonstrated potential as a material for wound closure and restoration.

Keywords

Carboxymethyl Chitosan/Tannins/Copper Ions, Hydrogel Excipients, Chronic Wounds

1. Introduction

As the global population ages, the prevalence of chronic wounds is rising annually. Studies indicate that approximately 1% - 2% of the world's population is affected by chronic wounds, with over 6.5 million diagnosed cases in the United States alone [1] [2]. In addition to the burden on patients, chronic wounds have a significant economic impact, costing the US healthcare system over $20 billion per year [3]. Chronic wounds are highly susceptible to complications such as infections, and in more severe cases, can lead to amputation or patient mortality due to unmanaged soft tissue damage if not properly treated and cared for [4]. Currently, the treatment of chronic wounds remains a significant challenge in clinical practice. Although some scholars have successfully treated certain patients using skin flaps and other surgical procedures, the majority of patients suffer from long-term illness, leading to poor surgical tolerance and high surgical risks. Therefore, conservative treatment methods, such as regular wound dressing changes, are still necessary [5]. With the gradual deepening of wound excipients research, more and more new excipients have been applied in the treatment of clinical chronic wounds, such as hydrogel excipients, seaweed excipients, etc. However, contemporary clinical excipients exhibit limited antibacterial efficacy on wounds and are unable to effectively promote wound healing while preventing infections. Consequently, the therapeutic outcomes for conservatively managed chronic wounds using these excipients are suboptimal.

Copper, as an antimicrobial metal, has a long history in the antimicrobial field, and it also plays a vital role in the process of wound healing, especially showing remarkable effects in promoting collagen synthesis and accelerating angiogenesis. Copper ions can not only facilitate the synthesis of collagen within the wound through their catalytic effect but also regulate multiple growth factors, promote angiogenesis, and accelerate tissue repair. Furthermore, copper ions possess a potent antibacterial property, which can effectively eliminate bacteria on the wound surface, prevent infection, and thereby further promote wound healing [6]. In addition to the general antimicrobial properties of other antimicrobial metals, they have gained attention due to their low price. Materials containing copper have excellent antimicrobial properties as demonstrated by Warnes S.L. *et al.* [7] when bacteria were spread on untreated brass, the bacteria were killed off after 7 hours and when bacteria were applied to the area where new brass was exposed after rubbing, the time of bacterial death was reduced to 15 minutes, proving the excellent antimicrobial properties of copper.

To address the limitations of conventional wound aids, such as inadequate antimicrobial properties and limited capacity to promote wound healing, this study developed an antimicrobial, stable, and effective hydrogel excipient for the closure and repair of skin wounds. The tannic acid/copper ion hydrogel excipient has outstanding antimicrobial properties and this topological adhesion allows the hydrogel to form a strong adhesion with the tissue without any chemical reaction with the tissue. By leveraging molecular entanglement and hydrogen bonding, the toughness of hydrogels can be significantly improved with the incorporation of carboxymethyl chitosan. The hydrogel's remarkable versatility and resilience effectively inhibit bacterial infection, facilitate tissue fluid absorption, and enhance the healing process of wounds. Consequently, it possesses significant potential as a wound dressing for promoting wound recovery.

2. Materials and Methods

2.1. Preparation of Hydrogel Dressings

2.1.1. Preparation of Tannic Acid/Copper Ion (TA/Cu^{2+}) Composite Nanoparticles

Equal masses of TA (tannic acid, Maclean's, CAS: 1401-55-4) and $CuSO_4$-$5H_2O$ (copper sulphate pentahydrate, Aladdin's, CAS: 7758-99-8) were weighed and dissolved in deionised water, and a small amount of ammonia (28 wt%) was gradually introduced into the tannic acid solution until it reached an alkaline state, and thorough agitation was applied. The tannic acid solution was subjected to dropwise addition of $CuCl_2$ solution, resulting in the formation of a precipitate. The obtained precipitate was then subjected to centrifugation at 5000 rpm for ten minutes, followed by three washes with deionised water and subsequent freeze-drying. This process led to the production of composite nanoparticles consisting of tannic acid and copper ions (TA/Cu^{2+}). The precipitate was collected, and then the precipitate was washed three times with alkaline water at pH = 8.0 until the supernatant approximated the state of deionised water. The dispersion was kept in alkaline water with pH = 8.0 at 4˚C for storage in order to prepare homogeneous and stable TA/Cu^{2+} nanoparticles.

2.1.2. Preparation of CMCS-TA/Cu^{2+} Hydrogel Dressings

A certain mass of CMCS (carboxymethyl chitosan, Maclean's, CAS: 83512-85-0) was weighed, fully dissolved, and prepared to 2% concentration. Tannic acid/copper ion (TA/Cu^{2+}) composite nanoparticles were incorporated into the CMCS solution, mixed homogeneously, and freeze-dried; the concentrations of tannic acid/copper ion (TA/Cu^{2+}) composite nanoparticles in the solution were 10%, 15%, and 20%, and were named as CMCS-TA/Cu^{2+}-10%, CMCS-TA/Cu^{2+}-15%, CMCS-TA/Cu^{2+}-20%; the water-soluble CMCS can anchor the TA/Cu^{2+} composite nanoparticles in the CMCS gel network to prepare antibacterial, antioxidant, and tube-enabling wound dressings.

2.2. Hydrogel Physicochemical Property Testing

2.2.1. Scanning Electron Microscopy, Infrared and XRD Characterisation of CMCS-TA/Cu^{2+} Determination

The hydrogels underwent freeze-drying followed by gold spraying, and the microscopic structure of the substances was examined using a SU9000 scanning electron microscope. TA, TA/Cu^{2+} and CMCS, CMCS-TA/Cu^{2+}-10%, CMCS-TA/Cu^{2+}-15%, CMCS-TA/Cu^{2+}-20% were detected using a Fourier infrared spectrometer (MAGNA560, Nicolet, USA) with a measuring range of 500 - 4000 cm^{-1}. The results of CMCS, TA/Cu^{2+} and CMCS, TA/Cu^{2+}-10%, CMCS-TA/Cu^{2+}-15%, CMCS-TA/Cu^{2+}-20% were measured on a Shimadzu XRD6000 diffractometer for CMCS, TA/Cu^{2+}, the XRD patterns of CMCS-TA/Cu^{2+} were obtained using a test voltage of 40 kV, with measurements taken within the 2θ range from 5˚ to 60˚ and at a scanning rate of 0.02˚/min.

2.2.2. Dissolution Rate and Porosity Testing of CMCS-TA/Cu^{2+}

The hydrogels' swelling characteristics were investigated using gravimetric analysis. The hydrogels underwent freeze-drying and their weight (W_d) was measured, followed by immersion in water for infiltration. When the swelling reached equilibrium, the excess surface water was removed using filter paper and its weight (W_s) was documented The rate of dissolution was obtained using Equation:

$$\text{Swelling ratio (\%)} = W_s - W_d / W_d \times 100\%$$

The determination of porosity was conducted using the liquid substitution technique, where ethanol was employed as the substituting liquid. In brief, a specific quantity of freeze-dried hydrogel was submerged in ethanol until it reached saturation point within the hydrogel. After 24 h, the material was removed and weighed (W_2).

The porosity (P) is calculated by the following Equation:

$$P = (W_2 - W_1)/(\rho V_1)$$

Let W_1 and W_2 represent the weight of the hydrocolloid prior to and following immersion, correspondingly. V_1 denotes the volume of alcohol before immersion, while ρ represents the constant density of alcohol.

2.2.3. DPPH Antioxidant Assay

The hydrogel's antioxidant property was assessed by measuring its ability to scavenge free radicals using the *in vitro* DPPH method. An amount of 3 mg of lyophilized hydrogel substance was introduced into a 4ml solution containing DPPH in methanol at a concentration of 100 μM, followed by incubation for a specific duration under light-protected conditions, The absorbance Ac of the solution at 517 nm was determined using a UV spectrophotometer. To establish a blank control, the absorbance As of the DPPH solution without any additional material was determined, and the absorbance A_s was calculated by using Equation. The calculation of the rate at which free radicals are scavenged was performed using Equation:

$$\text{DPPH scavening (\%)} = A_s - A_c / A_c \times 100\%$$

2.2.4. *In Vitro* Release Assay of Cu^{2+}

In order to elicit the release of copper ions *in vitro*, a specific amount of freeze-dried hydrogel was submerged in 0.1 m phosphate buffered saline (pbs) and maintained at 37˚C for a limited duration (ranging from 1 to 14 days). The ICP Inductively Coupled Plasma Spectrometer was utilized to analyze the ion concentration and determine the cumulative release concentration of copper ions by examining the solution containing released ions.

2.3. Animal Experiments

2.3.1. Animals

SPF grade 12-week-old SD rats, with a weight range of 220 to 250 g, were acquired from the animal laboratory of Southern Medical University and approved by the Animal Ethics Committee. The experimental animals were accommodated in the standardised animal facility at Southern Medical University, where the indoor temperature ranged from 18˚C to 22˚C, relative humidity was maintained between 40% and 70%, and ample lighting was provided. The experimental animals were pre-housed for 3 days after arrival at the animal house for formal experiments.

2.3.2. Chronic Wound Modelling and Hydrogel Dressing Application

Experimental animals were anesthetized with 3% pentobarbital sodium at a dose of 30 mg/kg. After abdominal injection of anesthesia, SD rats were placed on sterile surgical pads after entering the anesthetic state 2 - 3 min later. The hair shaver on the back of SD rats was removed, the skin on the back was exposed, and fixed on the rat table. The back of SD rats was thoroughly disinfected with iodine, and 4 round full-layer skin defects with a diameter of 5 mm were created on the back of SD rats with a round animal skin punch [8]. The untreated left side of their back wounds was designated as a blank control group (control group). The hydrogel experimental group (hydrogel group) utilized CMCS-TA/Cu^2 hydrogel to close the wound on the right side of the back. Using a digital camera, the hydrogel adjuvant was changed and wound closure was assessed on days 3, 6 and 12. The calculation formula for Wound area closure rate is as follows: Wound area closure ratio (%) = $W_0 - W_N / W_0 \times 100\%$. In the above formula, W_0 represents the size of the back wound area of SD rats on the day of surgery, that is, day 0, and W_n represents the size of the back wound area of SD rats on the day n after surgery.

2.4. Data Statistics and Analyses

The statistical analysis involved conducting ANOVA test, followed by Tukey's multiple comparisons test. GraphPad Prism, version 7.0 was utilized for this purpose.

3. Results

3.1. Scanning Electron Microscopy Characterisation of CMCS-TA/Cu^{2+}

The scanning electron microscopy was utilized to observe the microscopic structure of CMCS-TA/Cu^{2+} hydrogels with varying ratios. From **Figure 1**, it was found that the interconnectivity between the pores of CMCS-TA/Cu^{2+} hydrogels was observed. With the incorporation of TA/Cu^{2+} nanoparticles, there was a slight alteration observed in the pore size of the hydrogels, indicating that CMCS and TA/Cu^{2+} nanoparticles underwent hydrogen-bonding cross-linking, with the degree of cross-linking gradually increasing and the pore size becoming smaller.

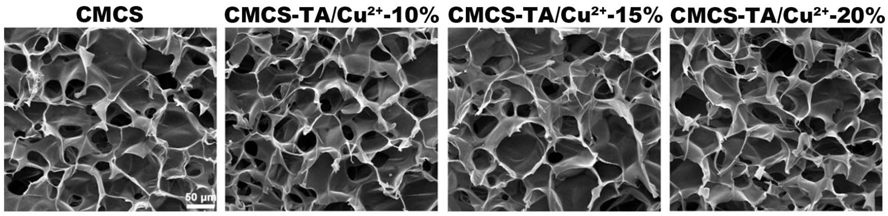

Figure 1. Scanning electron microscopy characterisation of CMCS-TA/Cu^{2+}.

3.2. Infrared Characterisation Test Results

In Fourier transform infrared spectroscopy (FTIR), a new vibrational peak at 1509.05 cm^{-1}, *i.e.*, a change in the HO-C stretching peak, was observed in TA/Cu^{2+} compared to TA; another vibrational peak near 3000 - 3500 cm^{-1} attributed to the phenolic hydroxyl group on the benzene ring was altered in TA/Cu^{2+}, indicating that there is an effective coordination between phenolic hydroxyl groups and copper ions. There exists a well-coordinated interaction between the phenolic hydroxyl group and the copper ion.

The interaction between CMCS and TA/Cu^{2+}, including the formation of hydrogen bonds, was investigated using ATR-FTIR; regarding the FTIR spectra of CMCS, suggesting that the peaks at 3000 - 3600 cm^{-1} correspond to the hydroxyl and amino group stretching vibrations, and the peaks at 3000 - 2800 cm^{-1} belong to the -CH stretching vibration. The carboxyl group (-COOH) exhibited absorption peaks at 1578.45 cm^{-1} and 1402 cm^{-1}, corresponding to the asymmetric and symmetric stretching vibrations, respectively. The characteristic absorption peaks of carboxyl group at 1578.45 cm^{-1} and 1402 cm^{-1} were weakened by the addition of TA/Cu^{2+}, which verified the cross-linking TA/Cu^{2+} as well as CMCS (**Figure 2**).

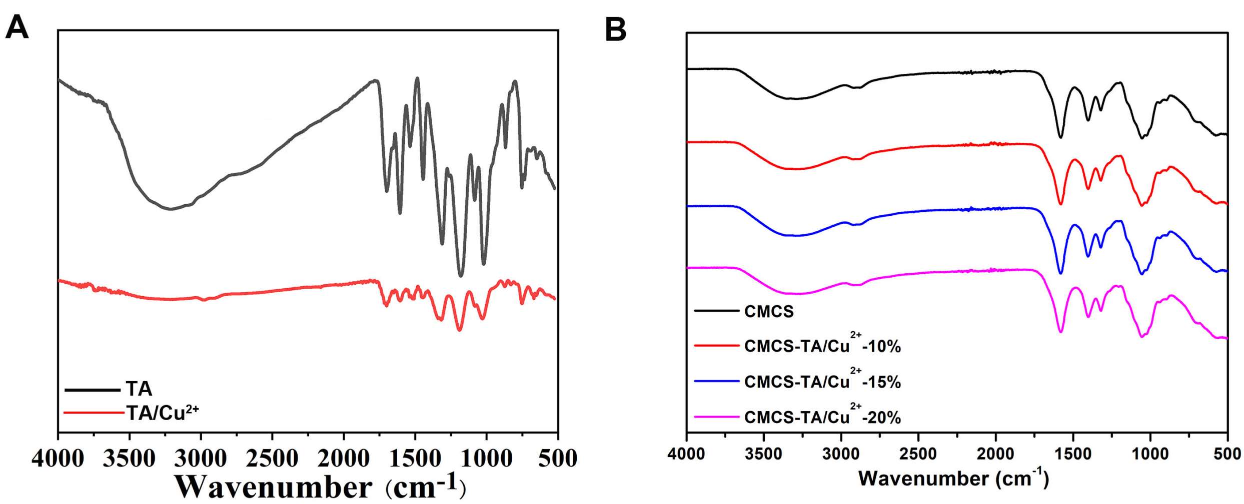

Figure 2. IR characterisation of TA, TA/Cu^{2+} (A); CMCS, CMCS-TA/Cu^{2+} (B).

3.3. XRD Characterisation Test Results

The XRD patterns of TA/Cu^{2+} and CMCS exhibit peaks with an amorphous "bun" shape, suggesting the presence of structures lacking long-range order. With the introduction of TA/Cu^{2+} and CMCS cross-linking, the XRD patterns of CMCS-TA/Cu^{2+} exhibited a reduction in intensity for characteristic peaks at $2\theta = 20^\circ$ - 30° compared to TA/Cu^{2+}. Additionally, there was a noticeable shift in peak positions. This phenomenon can be attributed to the further decrease in exposed phenolic groups within TA/Cu^{2+} due to its cross-linking with CMCS. The XRD patterns of the characteristic peak intensities for CMCS-TA/Cu^{2+} and CMCS with loading percentages of 10%, 15%, and 20% exhibited no significant disparities, suggesting that TA/Cu^{2+} successfully penetrated the gel interlayer and potentially achieved uniform dispersion within the micron-scale gel system (**Figure 3**).

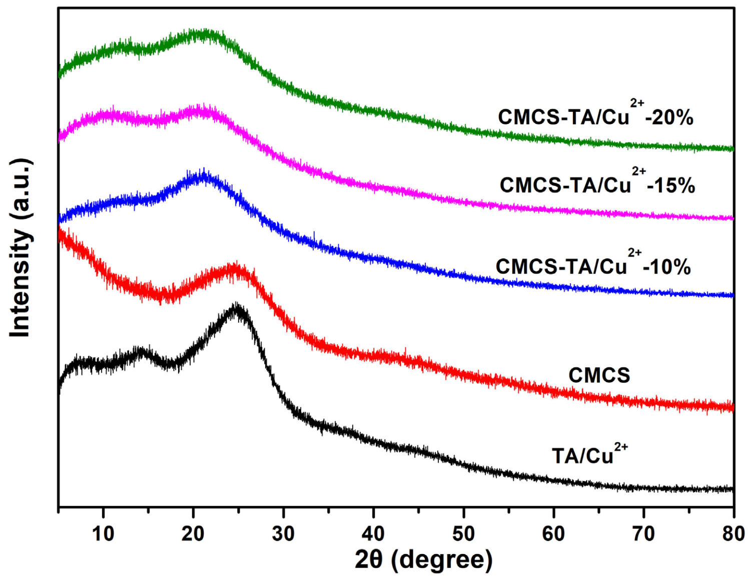

Figure 3. XRD characterisation of the CMCS-TA/Cu^{2+}.

3.4. Dissolution Rate and Porosity Test Results of CMCS-TA/Cu^{2+}

The CMCS hydrogel exhibited exceptional water absorption and storage capacity, as evidenced by its swelling rate of 747%. The hydrogels composed of CMCS-TA/Cu^{2+} exhibited swelling ratios of 1552%, 1173%, and 838% at different proportions (10%, 15%, and 20%) respectively. Notably, the hydrogel composed of CMCS-TA/Cu^{2+} exhibited a decrease in swelling rate as the dosage of TA/Cu^{2+} increased. The addition of TA/Cu^{2+} resulted in the cross-linking of hydrogen bonds between CMCS and TA/Cu^{2+}, which led to an increase in the cross-linking degree of the gel, a decrease in the pore size, and a decrease in the water-absorbing capacity of the CMCS-TA/Cu^{2+} hydrogel (**Table 1**).

The alcohol displacement method was employed to determine porosity. CMCS exhibited a porosity ranging from 84% to 93% of the total volume, while the porosity of the hydrogel doped with TA/Cu^{2+} in CMCS-TA/Cu^{2+} varied between 75% and 87%. Compared to the CMCS control, the reduction in sample porosity did not exhibit a substantial difference. The reduction in porosity resulted from the interplay between TA/Cu^{2+} ions and CMCS. Ethanol was employed as a solvent due to its inability to dissolve the freeze-dried configuration of CMCS hydrogels.

The pore size of the hydrogel plays a significant role in determining porosity, which in turn affects the material's capacity to absorb wound exudate or facilitate the transportation of nutrients and oxygen. Fluid absorption helps to control infection at the wound site (Figure 4).

Table 1. Swelling parameters of the various hydrogel.

	Swelling parameters of the gel system					
	Gt (min)	% Seq	ria	kAb	Smax	% EWC
CMCS	60	155	0.00722	3.21×10^{-3}	195	747
10% CMCS-TA/Cu^{2+}	60	437	0.00256	1.73×10^{-3}	462	1552
15% CMCS-TA/Cu^{2+}	60	698	0.00476	4.98×10^{-5}	627	1552
20% CMCS-TA/Cu^{2+}	60	533	0.00366	2.67×10^{-3}	289	838

*Gt, start-time of gel formation; % Seq, equilibrium swelling; ria, initial swelling rate; kA, swelling rate constant; % EWC, equilibrium water content. **a (g water/g gel)/min, b (g gel/g water)/min.

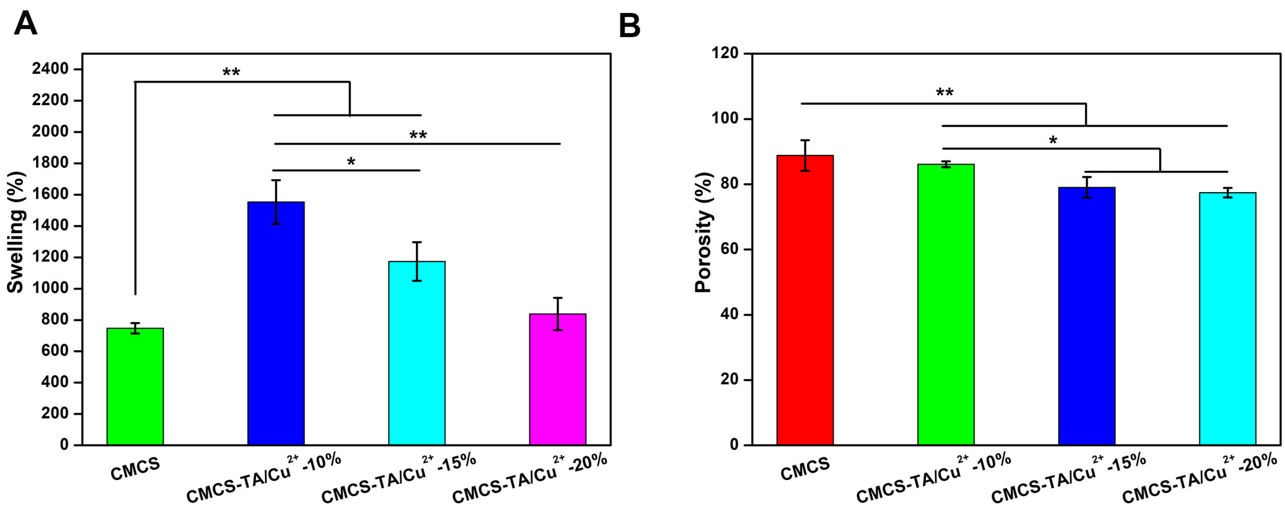

Figure 4. Solubility (A) and porosity (B) of CMCS-TA/Cu^{2+}.

3.5. Results of DPPH Antioxidant Experiments

The hydrogel's capacity to scavenge the stable free radical DPPH was assessed as a measure of its antioxidant potential. The findings revealed that the DPPH absorption peak at 516 nm of CMCS exhibited a negligible difference compared to the blank group, suggesting that the antioxidant property of CMCA was minimal. The increase in the content of TA/Cu^{2+} led to a noticeable decrease in the intensity of the DPPH absorption peak at 516 nm, resulting in an enhanced radical scavenging effect. Within a time frame of 5 minutes, the CMCS-TA/Cu^{2+}-20% group exhibited a significant increase of up to 60% in its ability to scavenge free radicals. Similarly, both the CMCS-TA/Cu^{2+}-10% and CMCS-TA/Cu^{2+}-20% material groups demonstrated notable rates of free radical scavenging at 60% and 83%, respectively. It shows that the hydrogel has good free radical scavenging effect, *i.e.*, antioxidant property, which can reduce ROS and promote tissue repair (Figure 5).

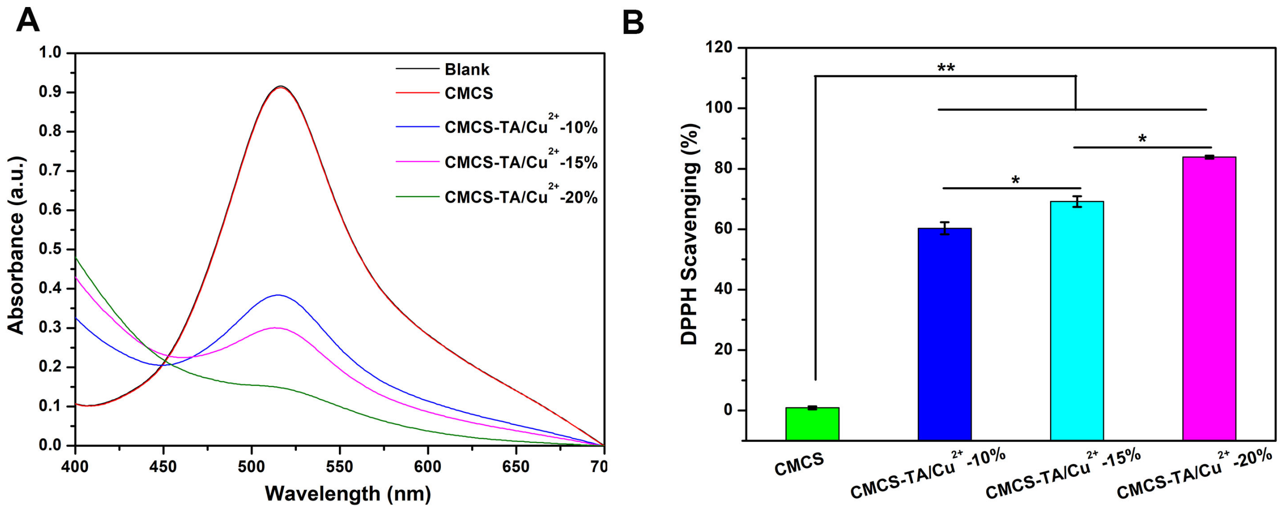

Figure 5. DPPH antioxidant assay (A) UV full spectrum of DPPH radical scavenging capacity of CMCS-TA/Cu^{2+}, (B) DPPH radical scavenging efficiency of CMCS-TA/Cu^{2+}.

3.6. *In Vitro* Release Assays for Cu^{2+}

The release profiles of copper ions from various hydrogel materials are depicted in figure. The release of copper ions increased proportionally with the increase in TA/Cu^{2+} content, which was an inevitable result; it is worth noting that each proportion of hydrogel could continuously emit copper ions over the course of one week gradually, which gradually smoothed out, suggesting that the hydrogel containing CMCS-TA/Cu^{2+} demonstrates enhanced efficacy in achieving sustained drug release. One possible explanation is that the strong bonding between CMCS and TA/Cu^{2+} through numerous hydrogen bonds allows for a stable release of CMCS-TA/Cu^{2+} over an extended period, thereby enabling sustained effectiveness of TA/Cu^{2+} for more than a week (**Figure 6**).

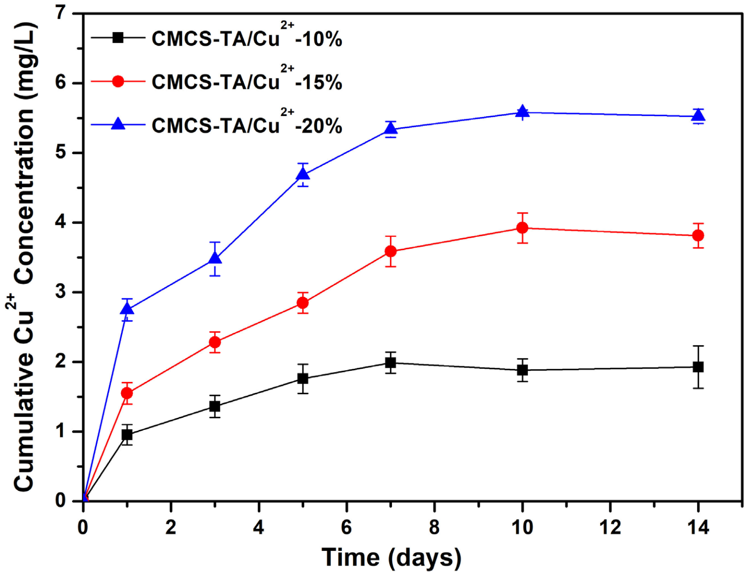

Figure 6. *In vitro* release of Cu^{2+}.

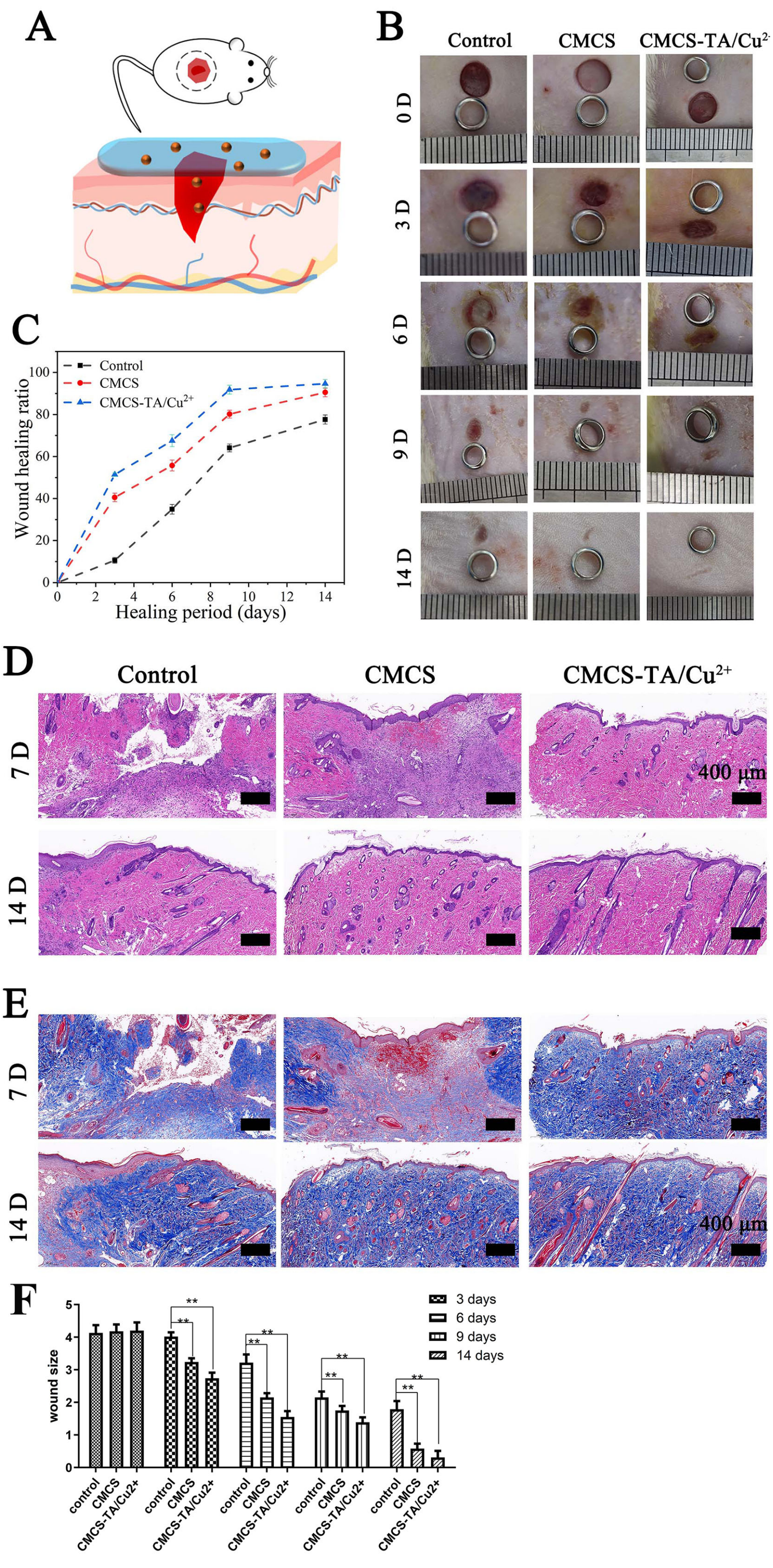

Figure 7. (A) Rat wound model; (B) A general view of the appearance of the wound at different time points; (C) Wound healing ratio on day 3, 6, 9, and 14d; (D) H&E and Masson staining for different groups (scale: 500 μm); (E) Wound size on day 3, 6, 9, and 14 d.

3.7. Rate of Healing in Rats with Chronic Wounds

A full-layer wound defect was modelled (**Figure 7(A)**). The wound healing process was assessed on days 3, 6, and 12. Wound area was significantly reduced in all groups during the longer treatment period. In particular, wound healing was significantly faster in the group treated with CMCS-TA/Cu^{2+} hydrogel than in the other group (**Figure 7(B)**, **Figure 7(C)**). The wound healing process was observed by H&E and Masson stained tissue sections, as shown in **Figure 7(D)**, **Figure 7(E)**, on the seventh day of the healing process, both groups exhibited a localized thickening of skin at the wound site that was found to be significantly greater than that of the surrounding skin, and the surface of the wounds was covered with large scabs, which could be seen to be filled with granulation tissue hyperplasia of the wounds, and there was a significant presence of numerous capillaries and infiltration of inflammatory cells observed within the granulation tissue. However, recovery of wounds demonstrated superior outcomes in the hydrogel group compared to the control group. On the 14th day of wound healing, the wound in the control group remained marginally more elevated compared to the skin. Epidermal regeneration was completed as well as regeneration of dermal glandular cavities was evident. In the hydrogel group, complete healing of the skin wound was observed, with well-organized regeneration of the glandular cavity and surrounding tissues without any noticeable harm. Additionally, there was evidence of inflammatory cell infiltration in the vicinity of the wound. Consequently, the hydrogel group exhibited superior wound healing in comparison to the control group.

4. Discussion

The skin, as the largest organ of the human body, serves as a vital protective barrier. It plays an indispensable role in defending against external harmful environments and toxic substances, preventing bacterial infections, and minimizing water and electrolyte loss [9]. Loss of skin integrity due to various reasons is highly susceptible to microbial infections, especially in chronic wounds, making the treatment of chronic wounds one of the clinical challenges [10]. In chronic wounds, bacteria develop a biofilm that encapsulates them during proliferation, thereby hindering the penetration of antimicrobial agents and compromising their efficacy. Relying on debridement alone does not completely remove the bacteria and their biofilm, resulting in recurrence of infection and prolonged healing of the wound [11]. While antibiotic therapy can effectively inhibit bacterial proliferation and complement debridement, prolonged use of broad-spectrum antibiotics may readily lead to multidrug resistance in bacteria. This complicates the clinical management of infected wounds [12] [13].

Wound dressings are considered the most direct and effective method of wound care. However, traditional wound dressings have only a single function of physical barrier or exudate absorption, and are weak in promoting healing. In addition, these dressings may even lead to re-injury during use, increasing treatment costs and patient burden [14]. Therefore, ideal dressings should not only absorb wound exudate and keep the wound moist, but also have good antimicrobial properties [13]. In this study, the hydrogel excipients constructed on the basis of CMCS, TA, and Cu^{2+} were tested by universal testing machine, Fourier infrared spectrometer, scanning electron microscope, and testing the mechanical properties, functional group changes, morphological characteristics and stability of hydrogels, and the degradation and swelling of hydrogels were also investigated, showing that the hydrogels CMCS/TA/Cu^{2+} hydrogels have a three-dimensional porous structure, good TA/Cu^{2+} has good porosity which facilitates the exchange of oxygen and nutrients and promotes cell proliferation. CMCS/TA/Cu^{2+} Hydrogel provides a relatively complete protective barrier against external damage during the initial stages of wound healing and reduces the risk of wound infection. It does not need to be removed or moved after the wound has healed, which can prevent secondary injuries from occurring. Meanwhile, Cu^{2+} can play an effective antibacterial role in reducing the occurrence of wound infection. In the rat model, the application of CMCS/TA/Cu^{2+} hydrogel can significantly accelerate the healing process of the wound, meanwhile, it has good biocompatibility and avoids the damage of immune response to the wound.

In conclusion, the multifunctional hydrogel prepared in this study has good physicochemical and biological properties, which can effectively kill bacteria, remove bacterial biofilm and promote the healing of infected wounds. It is a new candidate for wound dressing application. This dressing may bring a new choice for the treatment of chronic wounds such as diabetic foot. However, since this dressing is still in the experimental research stage, the real effect of this dressing on patients needs to be further verified.

Funding

Foundation of Science and Technology Projects in Guangzhou (2024A03J1061).

Conflicts of Interest

The authors declare no conflicts of interest regarding the publication of this paper.

References

[1] Domingues Paulino, R. and Williams, J.M. (2023) Chronic Axillary Wounds in Cats: What Do We Know and How Should We Manage Them? *Journal of Feline Medicine and Surgery*, **25**. https://doi.org/10.1177/1098612x231162880

[2] Wilkinson, H.N. and Hardman, M.J. (2020) Wound Healing: Cellular Mechanisms and Pathological Outcomes. *Open Biology*, **10**, Article ID: 200223. https://doi.org/10.1098/rsob.200223

[3] Sun, H., Pulakat, L. and Anderson, D.W. (2020) Challenges and New Therapeutic Approaches in the Management of Chronic Wounds. *Current Drug Targets*, **21**, 1264-1275. https://doi.org/10.2174/1389450121666200623131200

[4] Graves, N., Phillips, C.J. and Harding, K. (2021) A Narrative Review of the Epidemiology and Economics of Chronic Wounds. *British Journal of Dermatology*, **187**, 141-148. https://doi.org/10.1111/bjd.20692

[5] Zindle, J.K., Wolinsky, E. and Bogie, K.M. (2021) A Review of Animal Models from 2015 to 2020 for Preclinical Chronic Wounds Relevant to Human Health. *Journal of Tissue Viability*, **30**, 291-300. https://doi.org/10.1016/j.jtv.2021.05.006

[6] Bonetta, R. (2017) Potential Therapeutic Applications of MnSODs and SOD-Mimetics. *Chemistry—A European Journal*, **24**, 5032-5041. https://doi.org/10.1002/chem.201704561

[7] Fino, P., Di Taranto, G., Pierro, A., Kacjulite, J., Codolini, L., Onesti, M.G., Toscani, M. and Tarallo, M. (2019) Depression Risk among Patients with Chronic Wounds. *European Review for Medical and Pharmacological Sciences*, **23**, 4310-4312.

[8] Song, Y., You, Y., Xu, X., Lu, J., Huang, X., Zhang, J., *et al.* (2023) Adipose-derived Mesenchymal Stem Cell-derived Exosomes Biopotentiated Extracellular Matrix Hydrogels Accelerate Diabetic Wound Healing and Skin Regeneration. *Advanced Science*, **10**, e2304023. https://doi.org/10.1002/advs.202304023

[9] Cross, K. and Harding, K. (2022) Risk Profiling in the Prevention and Treatment of Chronic Wounds Using Artificial Intelligence. *International Wound Journal*, **19**, 1283-1285. https://doi.org/10.1111/iwj.13952

[10] Kaushik, K. and Das, A. (2019) Endothelial Progenitor Cell Therapy for Chronic Wound Tissue Regeneration. *Cytotherapy*, **21**, 1137-1150. https://doi.org/10.1016/j.jcyt.2019.09.002

[11] Kodange, C. (2021) Screening for Depression in Patients with Chronic Wounds. *Advances in Skin & Wound Care*, **34**, 502-503. https://doi.org/10.1097/01.asw.0000767380.11275.88

[12] Cheung, C. (2010) Older Adults and Ulcers: Chronic Wounds in the Geriatric Population. *Advances in Skin & Wound Care*, **23**, 39-44. https://doi.org/10.1097/01.asw.0000363487.01977.a9

[13] Huang, Z., Wu, S., Yu, T. and Hu, A. (2021) Efficacy of Telemedicine for Patients with Chronic Wounds: A Meta-Analysis of Randomized Controlled Trials. *Advances in Wound Care*, **10**, 103-112. https://doi.org/10.1089/wound.2020.1169

[14] Kolimi, P., Narala, S., Nyavanandi, D., Youssef, A.A.A. and Dudhipala, N. (2022) Innovative Treatment Strategies to Accelerate Wound Healing: Trajectory and Recent Advancements. *Cells*, **11**, Article 2439. https://doi.org/10.3390/cells11152439